

1 **Title:** VAMP711 is required for abscisic acid-mediated inhibition of plasma
2 membrane H⁺-ATPase activity

3

4 **Short title:** VAMP711 regulates plasma membrane H⁺-ATPase activity

5

6 Yuan Xue, Yongqing Yang, Zhijia Yang, Xiangfeng Wang, Yan Guo*

7

8 State Key Laboratory of Plant Physiology and Biochemistry, College of
9 Biological Sciences, China Agricultural University, Beijing, China

10

11 **Keywords:** PM H⁺-ATPase, drought stress, ABA, stomatal closure,
12 Arabidopsis

13

14 Author for Contact / Senior Author:

15 Yan Guo

16 E-mail: guoyan@cau.edu.cn

17 Phone: 86-10-62732030

18 Fax: 86-10-62732030

19

20

21 **One-sentence summary:** The SNARE protein VAMP711 is involved in
22 regulating abscisic acid-mediated inhibition of plasma membrane H⁺-ATPase
23 activity in response to drought stress.

24

25 **Author contributions:**

26 Y.G. and Y.X. conceived and designed the research plans; Y.X. and Z.Y.

27 performed the experiments; Y.G., Y.X., Y.Y. and X.W. analyzed data. Y. G., Y. X.

28 and Y.Y. wrote the paper.

29 **ABSTRACT**

30 Drought stress is a limiting environmental factor that affects plant growth and
31 development. The plant hormone abscisic acid (ABA) plays an important role
32 in plant drought responses. Previous studies have indicated that ABA inhibits
33 plasma membrane H⁺-ATPase (PM H⁺-ATPase) activity, and the decrease in
34 PM H⁺-ATPase activity promotes stomatal closure under drought stress,
35 thereby reducing water loss. However, the underlying molecular mechanisms
36 are not well understood. In this study, we found that in *Arabidopsis thaliana*
37 ABA induces an *N*-ethylmaleimide-sensitive factor attachment protein receptor
38 (SNARE) protein, namely, VESICLE-ASSOCIATED MEMBRANE PROTEIN
39 711 (VAMP711) to interact with the Arabidopsis PM H⁺-ATPases AHA1 and
40 AHA2. The interaction occurs at their C-termini and inhibits PM H⁺-ATPase
41 activity. Deletion of *VAMP711* in Arabidopsis results in a higher PM H⁺-ATPase
42 activity and slower stomatal closure in response to ABA and drought
43 treatments. In addition, overexpression of *VAMP711* partially rescues the
44 drought-sensitive phenotype of *ost2-2D*, a mutation in *AHA1* resulting in a
45 constitutive activated PM H⁺-ATPase. Our results demonstrate that VAMP711
46 is involved in regulating ABA-mediated inhibition of PM H⁺-ATPase activity and
47 stomatal closure in response to drought stress.

48 INTRODUCTION

49 Plasma membrane (PM) H⁺-ATPase regulates many cellular activities by
50 producing electrochemical gradients across the plasma membrane. Therefore,
51 the activity of PM H⁺-ATPase must be tightly controlled. In plants, PM
52 H⁺-ATPase plays regulatory roles in many cellular and development processes,
53 such as cell expansion, intracellular pH homeostasis, and response to saline
54 and drought stresses (Fuglsang et al., 2007; Merlot et al., 2007; Palmgren,
55 2001; Roberkleber et al., 2003; Yamauchi et al., 2016; Yang et al., 2010). The
56 *Arabidopsis thaliana* genome contains 11 PM H⁺-ATPase genes (*AHA1* to
57 *AHA11*) (Falhof et al., 2016; Haruta et al., 2017; Palmgren, 2001).

58 The C-terminus (~100 residues) of PM H⁺-ATPase contains the
59 autoinhibitory domain of the enzyme activity (Palmgren et al., 1991). The
60 phosphorylation of the C-terminus is critical for the regulation of PM
61 H⁺-ATPase activity. The phosphorylation of the penultimate residue (Thr-947)
62 of AHA2 generates a 14-3-3 binding site to activate PM H⁺-ATPase activity
63 (Camoni et al., 2000; Gévaudant et al., 2007; Svennelid et al., 1999); the
64 phosphorylation of the C-terminus of AHA2 (Ser-931) by a Ser/Thr protein
65 kinase (PKS5) inhibits the interaction between AHA2 and 14-3-3 to decrease
66 PM H⁺-ATPase activity (Fuglsang et al., 2007; Kinoshita and Shimazaki, 2002;
67 Yang et al., 2010).

68 ABA negatively regulates PM H⁺-ATPase activity (Merlot et al., 2007). It
69 promotes the dephosphorylation of the Thr-947 site in AHA2 (Cai et al., 2017;
70 Falhof et al., 2016; Yin et al., 2013) and Snf1-related protein kinase 2.6
71 (SnRK2.6)/open stomata 1 (OST1) protein is involved in this regulation (Merlot
72 et al., 2007). SnRK2.2 but not SnRK2.6 directly phosphorylates the C-terminus
73 of AHA2 (Planes et al., 2015). The dominant mutants of *ost2-1D* and *ost2-2D*
74 (*AHA1*) show constitutive higher PM H⁺-ATPase activity and abolish guard cell
75 response to ABA (Merlot et al., 2007). However, the underlying molecular
76 mechanisms are not well understood.

77 In addition to the regulation of PM H⁺-ATPase activity by direct phosphorylation,
78 the regulation of the amount of PM H⁺-ATPase protein is an important
79 mechanism that affects its activity (Hashimoto-Sugimoto et al., 2013).

80 H⁺-ATPase translocation control 1 (PATROL1) is a Munc13-like protein related
81 to synaptic vesicle priming (Basu et al., 2005), which regulates AHA1
82 translocation to the plasma membrane and mediates stomatal movement in
83 response to environmental signals such as light and CO₂
84 (Hashimoto-Sugimoto et al., 2013).

85 SNARE proteins play an essential role in vesicle trafficking by facilitating the
86 fusion of vesicles and the target membrane in eukaryotes (Uemura et al.,

87 2004). SNARE proteins are classified into R- and Q-types according to the
88 similarity and specific amino acid sequence (Uemura et al., 2005). One
89 R-SNARE protein and three Q-SNARE proteins form a complex to promote
90 membrane fusion (Jahn and Scheller, 2006; Pratelli et al., 2004).
91 Vesicle-associated membrane protein 7 (VAMP7)-like proteins are one group
92 of R-SNARE, which comprises two sub-groups: VAMP71 and VAMP72
93 (Sanderfoot, 2007). The structure of SNARE proteins is conserved: a longin
94 domain in the N-terminus, and a SNARE domain and a transmembrane
95 domain (TMD, which anchors SNARE proteins to the membrane) in the
96 C-terminus in plants (Hong, 2005; Uemura et al., 2004).

97 In Arabidopsis, VAMP7s are involved in endosome trafficking and are highly
98 conserved and localized to the vacuolar membrane and plasma membrane
99 (Hong, 2005; Uemura et al., 2004). Increasing evidence shows that
100 SNARE-mediated pathways are involved in response to biotic and abiotic
101 stresses in plants (Collins et al., 2003; Leshem et al., 2010; Leshem et al.,
102 2006; Sugano et al., 2016). In rice (*Oryza sativa*), the intracellular SNARE
103 protein, OsVAMP714, plays a role in resistance to rice blast disease (Sugano
104 et al., 2016). In Arabidopsis, the decreased expression of *VAMP711* inhibits
105 the fusion of vesicles to the tonoplast, resulting in plant tolerance to salt and
106 drought stresses (Leshem et al., 2010; Leshem et al., 2006). In general,
107 VAMP7-mediated cellular activities are linked to the function of vesicle fusion.
108 However, the SNARE protein VAMP721 interacts with and inhibits the activity
109 of inward-rectifying K⁺ channels KAT1 and KC1 to regulate the vegetative
110 growth of Arabidopsis (Zhang et al., 2015).

111 In this study, we identified a SNARE family protein, VAMP711, as a negative
112 regulator of PM H⁺-ATPase. VAMP711 directly interacted with and inhibited
113 AHA1 and AHA2 activity, and this interaction was induced by ABA treatment.
114 The drought-hypersensitive phenotype and ABA-mediated stomatal closure
115 defect of the *ost2-2D* mutant were partially reduced by overexpression of
116 *VAMP711*. Our results suggest that ABA-mediated PM H⁺-ATPase activity
117 inhibition occurs, at least partially, through the interaction between VAMP711
118 and AHA1/AHA2, and provide evidence for an ABA-mediated regulatory
119 mechanism for PM H⁺-ATPase activity.

120
121

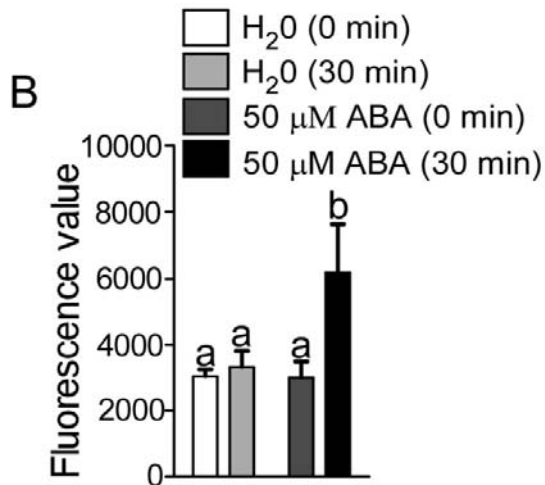
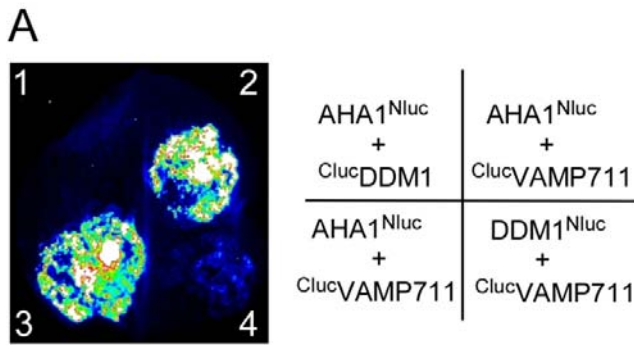
122 **RESULTS**

123 **VAMP711 interacts with PM H⁺-ATPase AHA1**

124 ABA inhibits PM H⁺-ATPase activity (Merlot et al., 2007; Planes et al., 2015).
125 To identify components involved in this inhibition, we first confirmed this result.
126 Four-week-old Arabidopsis Col-0 plants were treated with 200 mM NaHCO₃ for
127 2 days to induce PM H⁺-ATPase activity, and then treated with or without 10
128 μM of ABA for 1 day. The plasma membrane-enriched vesicles were isolated
129 and used for measuring PM H⁺-ATPase activity. The ABA treatment
130 significantly reduced H⁺-transport and ATP hydrolysis activities of PM
131 H⁺-ATPase (Supplemental Figures S1A to S1D). To identify possible regulators,
132 we generated more than 30 *Pro35S::GFP-AHA1* transgenic plants in Col-0 and
133 selected stable transgenic plants in which the GFP-AHA1 signal was localized
134 to the plasma membrane for further study. The 10-day-old transgenic plants
135 were treated with or without 50 μM of ABA for 6 hours, the plasma
136 membrane-enriched fraction was collected, the GFP-AHA1 was
137 immunoprecipitated with anti-GFP antibody–conjugated agarose, and putative
138 AHA1-interacting proteins were detected by mass spectrometry (MS). A
139 SNARE family protein, VAMP711, was identified as a putative
140 AHA1-interacting protein.

141 To verify this interaction, we performed luciferase complementation (LUC)
142 assay by constructing *AHA1^{Nluc}* and *ClucVAMP711* vectors, and transformed
143 them into *Nicotiana benthamiana* leaves to collect luminescence signals after
144 a 3-day incubation. The luminescence signal was detected in leaves
145 expressing *AHA1^{Nluc}* and *ClucVAMP711*; as a control, transformation of
146 *AHA1^{Nluc}* and *ClucDDM1* (DDM1, DECREASED DNA METHYLATION 1),
147 *DDM1^{Nluc}* and *ClucVAMP711* showed a very low signal (Figure 1A); however,
148 the indicated genes were detected in *N. benthamiana* leaves at similar levels
149 (Supplemental Figure S2A). We also cotransformed *ClucAHA1* and
150 *VAMP711^{Nluc}* into *N. benthamiana* leaves. The luminescence signal was not
151 detected after the 3-day incubation (Supplemental Figure S2B), possibly
152 because Nluc and Cluc are not close enough due to the specific fusion
153 position.

154 To determine whether the interaction between VAMP711 and AHA1 is
155 induced by ABA, the *N. benthamiana* leaves transformed with *AHA1^{Nluc}* and
156 *ClucVAMP711* were treated with or without 50 μM ABA for 6 hours, and the
157 fluorescence value was collected. The results showed that ABA could
158 significantly promote the interaction between VAMP711 and AHA1 (Figure 1B).
159 Together, these results suggest that the SNARE protein VAMP711 interacts
160 with AHA1 and the interaction is induced by ABA treatment.



161 To determine the possible subcellular location where these proteins interact,
 162 we constructed *AHA1*^{YCE} and *YNE*VAMP711, *AHA1*^{YNE} and *YCE*VAMP711 for
 163 bimolecular fluorescence complementation (BIFC) assay. The combinations of
 164 *AHA1*^{YCE} and *YNE*VAMP711, *AHA1*^{YCE} and *YNE*DDM1, *DDM1*^{YCE} and
 165 *YNE*VAMP711, *AHA1*^{YNE} and *YCE*VAMP711, *YCE*SYP22 and *YNE*VAMP711,
 166 *YCE*SYP22 and *YNE*DDM1 were transiently expressed in *N. benthamiana* leaves,
 167 respectively. The YFP (yellow fluorescent protein) fluorescence signal was
 168 detected by confocal microscopy in leaves of expressed *AHA1*^{YCE} and
 169 *YNE*VAMP711 and *AHA1*^{YNE}, *YCE*VAMP711 (Supplemental Figures S2C and
 170 S2D). The YFP signal partially co-localized with the signal of FM4-64 dye,
 171 which was used to label the plasma membrane and endosomes
 172 (Supplemental Figures S2C and S2D). VAMP711 has been reported to be a
 173 vacuolar membrane-localized protein and AHA1 is a plasma membrane
 174 located protein (Hashimoto-Sugimoto et al., 2013; Leshem et al., 2006).
 175 Consistent with these notions, our results showed that VAMP711
 176 predominately localized to the vacuolar membrane and prevacuolar
 177 compartments (PVCs) and AHA1 was localized to the plasma membrane
 178 (Supplemental Figures S2E and S2F). The fluorescence signal of

179 GFP-VAMP711 was not colocalized with FM4-64 dye-labeled plasma
180 membrane in the *ProUBQ10:GFP-VAMP711* transgenic seedlings without ABA
181 treatment. However, when the *ProUBQ10:GFP-VAMP711* transgenic seedlings
182 were treated with ABA, some weak fluorescence signal of GFP-VAMP711 was
183 detected on the plasma membrane, and the Pearson correlation coefficient
184 was much higher in *ProUBQ10:GFP-VAMP711* transgenic seedlings treated with
185 ABA (Supplemental Figure S2G). In addition, the result of plasma membrane
186 isolation and immunoblot analysis showed that the amount of VAMP711
187 proteins on the plasma membrane was greater in *ProUBQ10:GFP-VAMP711*
188 transgenic seedlings subjected to ABA treatment than in seedlings not
189 subjected to ABA treatment (Supplemental Figure S2H). These results
190 indicated that ABA treatment might affect the localization of VAMP711. On the
191 basis of these results, we speculated that the interaction between VAMP711
192 and AHA1 might partially occur on the plasma membrane.

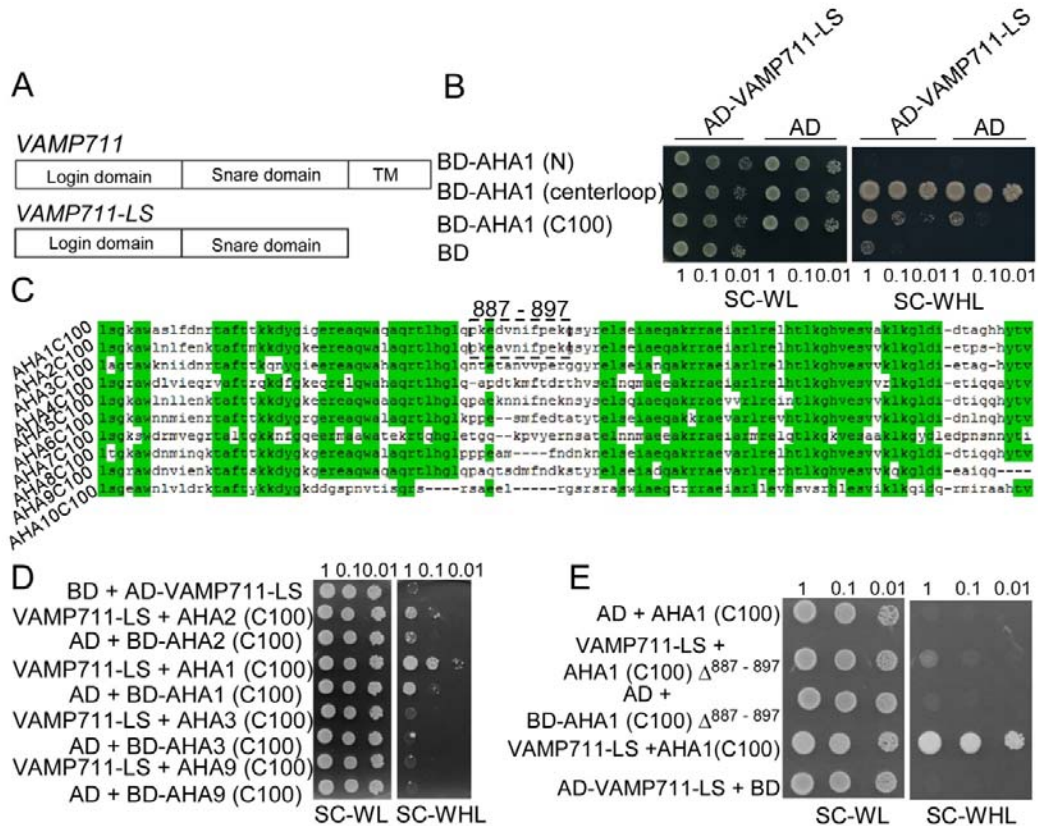
193

194 **VAMP711 interacts with the C-terminus of AHA1 and AHA2**

195 The SNARE protein VAMP711 has three conserved domains: the longin
196 domain, SNARE domain and transmembrane domain (Figure 2A) (Fujiwara et
197 al., 2014; Uemura et al., 2005), and AHA1 contains three intracellular parts:
198 N-terminus, centerloop and C-terminus (C100) (Falhof et al., 2016). We used
199 the VAMP711-LS (longin and SNARE domains of VAMP711) as a bait to detect
200 the VAMP711-interacting portion of AHA1 in the yeast two-hybrid system. The
201 indicated combinations were transformed into the yeast strain AH109. The
202 yeast cells containing pGBKT7-AHA1 (centerloop) and pGADT7 vector could
203 grow on synthetic complete (SC) medium lacking Trp, Leu and His (WHL). We
204 then tested the interaction between pGBKT7-AHA2 (centerloop) and
205 pGADT7-VAMP711-LS; and no interaction was detected (Supplemental Figure
206 S3B). The yeast cells containing the combinations of pGBKT7-AHA1 (C100)
207 and pGADT7-VAMP711-LS showed better growth than those containing the
208 combinations pGBKT7-AHA1 (C100) and pGADT7 on SC medium lacking
209 WHL. These results suggest that VAMP711 interacts with the C-terminus of
210 PM H⁺-ATPase (Figures 2A and 2B), which is a conserved domain (Figure 2C).

211 To determine the specificity of interaction, we co-transformed the
212 C-terminus of *AHA1*, *AHA2*, *AHA3* and *AHA9* with *VAMP711-LS* into a yeast
213 strain. Only *AHA1* and *AHA2* interacted with VAMP711 (Figure 2D). *AHA1* and
214 *AHA2* are two major members of the AHA family (Palmgren, 2001). We found
215 that 11 amino acid residues (887–897) in *AHA1* and *AHA2* are distinct from
216 those in other AHA members (Figure 2C). We speculated that these 11 amino
217 acid residues may be required for VAMP711 to interact with *AHA1* and *AHA2*

7



218 (Figure 2C). When the 11 residues in AHA1 and AHA2 were deleted, the
 219 interaction between AHA1 and VAMP711 was abolished (Figures 2E, S3A).
 220 Together, our results suggest that the interaction between the VAMP711 and
 221 the C-terminus of AHA1 and AHA2 requires these 11 amino acid residues.

222

223 VAMP711 negatively regulates PM H⁺-ATPase activity

224 To further investigate whether VAMP711 could regulate PM H⁺-ATPase activity
 225 by direct interaction, we generated two CRISPR/Cas9 *vamp711* mutants,
 226 *vamp711-6* and *vamp711-7*. A two-base deletion (GA, 98–99 bp) in the second
 227 exon was detected in the *vamp711-6* mutant, and one-base insertion (C
 228 between 16 and 17 bp) in first exon was detected in the *vamp711-7* mutant.
 229 Both these mutations led to frameshift and early termination of *VAMP711*
 230 (Supplemental Figure S4A).

231 We also constructed complementation lines of *vamp711-6* (*com-1*, *com-2*)
 232 by transferring a plasmid containing the *VAMP711* genomic sequence that
 233 included the promoter region (1,500 bp from the translational start site) and 3'
 234 untranslated region (500 bp downstream of the stop codon), more than 30
 235 transgenic plants were obtained and two independent T₄ transgenic lines
 236 (*com-1*, *com-2*) with *VAMP711* expression levels similar to those in the wild

237 type were used for further study (Supplemental Figure S4B).

238 We also generated *VAMP711*-overexpressing lines
239 (*Pro_{UBQ10}:GFP-VAMP711*) in the wild-type background and named these lines
240 *OE-VAMP711-15/27*. In the *OE-VAMP711* lines, the GFP-*VAMP711* signal was
241 localized at vacuolar membrane and prevacuolar compartments (PVCs).
242 Reverse-transcription PCR (RT-PCR) detected increased expression of
243 *VAMP711* in both overexpressing lines (Supplemental Figure S4C).

244 To investigate the PM H⁺-ATPase activity in Col-0, *vamp711-6*, *vamp711-7*,
245 and *OE-VAMP711-15/27*, we isolated plasma membrane vesicles from
246 4-week-old plants treated with 200 mM of NaHCO₃ for 3 days. The H⁺
247 transport activity in *vamp711-6/7* was 30% higher than that in Col-0; while the
248 activity in *VAMP711*-overexpressing lines were 10–15% lower than that in
249 Col-0 (Figures 3A and 3B). To detect the PM H⁺-ATPase protein level on the
250 plasma membrane in Col-0, *vamp711-6*, *vamp711-7*, and *OE-VAMP711-15/27*
251 plants under NaHCO₃ treatment, plasma membrane vesicles were isolated
252 and detected by immunoblotting with anti-PM H⁺-ATPase antibody. No obvious
253 difference was detected in Col-0, *vamp711-6*, *vamp711-7*, and
254 *OE-VAMP711-15/27* plants (Supplemental Figure S4D).

255 To further confirm the effect of *VAMP711* on H⁺ fluxes, the non-invasive
256 micro-test technique (NMT) was used to monitor H⁺ flux in the root.
257 Five-day-old seedlings of Col-0, *vamp711-6/7* and complementation lines
258 com-1/2 were incubated in buffer at pH 7.8 for 30 min; then, their root apices
259 were selected to detect the H⁺ flux for about 360 seconds. The H⁺ fluxes of
260 *vamp711-6/7* were significantly higher than those of Col-0 (Figures 3C and 3D).
261 There was no obvious difference in the H⁺ fluxes between com-1/2 lines and
262 the wild type (Supplemental Figures S4E and S4F). These results indicate that
263 *VAMP711* negatively regulates PM H⁺-ATPase activity in plants.

264 Arabidopsis mutants with a higher PM H⁺-ATPase activity display resistance
265 to high pH stress (Fuglsang et al., 2007; Yang et al., 2010). To investigate
266 whether mutation in *VAMP711* has a similar effect, we transferred 6-day-old
267 seedlings of Col-0, *vamp711-6/7* from MS medium at pH 5.8 to MS medium at
268 pH 5.8 or 8.0. There was no significant difference in the fresh weight and
269 primary root length of Col-0 and *vamp711-6/7* for one week after the transfer.
270 However, because of their PM H⁺-ATPase activity levels, the mutants of
271 *vamp711-6/7* were much more resistant to pH 8.0 than the wild type,
272 displaying higher fresh weight and longer primary root length for 10 days after
273 the transfer (Supplemental Figures S5A to S5C). These results further suggest
274 that *VAMP711* negatively regulates PM H⁺-ATPase activity.

275 To investigate whether *VAMP711* directly inhibits PM H⁺-ATPase activity, we

276 purified GST-tagged VAMP711-LS recombinant protein expressed in
277 *Escherichia coli* BL21. The PM H⁺-ATPase activity of the plasma membrane
278 vesicles was measured after incubation with 500 ng of VAMP711-LS
279 recombinant proteins for 15 min at room temperature. When VAMP711-LS
280 protein was added in the plasma membrane vesicles, H⁺-ATPase activity
281 decreased by about 20% compared to the activity observed when a negative
282 control or a GST protein was added (Figures 3E and 3F).

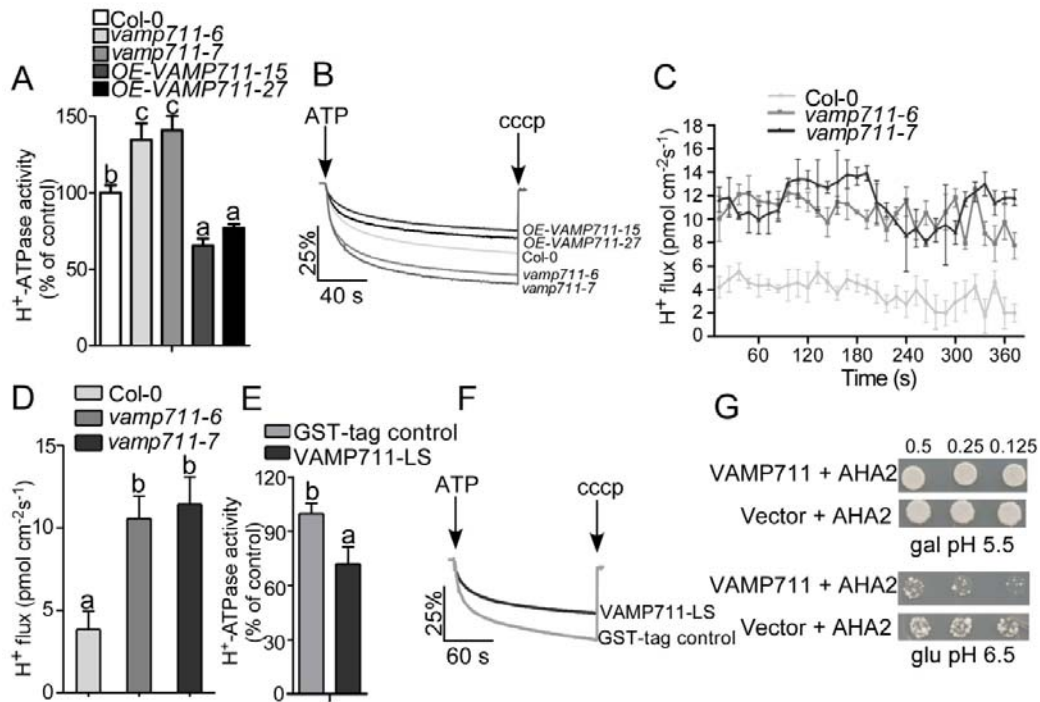
283 We then used the yeast strain RS72, the growth of which depends on
284 expressed heterologous AHA2 activity in glucose medium (Fuglsang et al.,
285 2007). We transferred VAMP711 into the RS72 yeast strain expressing
286 heterologous AHA2 to investigate the effect of VAMP711 on RS72 yeast
287 growth. The VAMP711 inhibited RS72 yeast growth on glucose medium at pH
288 6.5 (Figure 3G), which indicates that VAMP711 inhibits AHA2 activity. The
289 immunoblot analysis showed that the expression of VAMP711 did not affect the
290 PM H⁺-ATPase protein levels in the RS72 yeast strain (Supplemental Figure
291 S4G). Our results indicate that VAMP711 inhibits PM H⁺-ATPase activity by
292 direct interaction.

293

294 **VAMP711 is required for ABA-mediated inhibition of PM H⁺-ATPase** 295 **activity**

296 To study whether VAMP711 is required for ABA-mediated PM H⁺-ATPase
297 activity inhibition, we detected the H⁺ fluxes and PM H⁺-ATPase activity in
298 Col-0 and *vamp711* mutants under ABA treatment. The H⁺ influxes were not
299 obviously different between the *vamp711-6/7* mutants and the wild type not
300 subjected to ABA treatment (Figures 4A and 4B). The ABA treatment
301 significantly increased the H⁺ influxes in both Col-0 and *vamp711-6/7* mutants;
302 however, the H⁺ influxes in the seedlings of *vamp711-6/7* mutants were less
303 sensitive to ABA treatment than those in the wild-type seedlings (Figures 4C
304 and 4D). We then isolated the plasma membrane vesicles from 4-week-old
305 plants treated with or without 10 μM of ABA and measured the PM H⁺-ATPase
306 activity. The PM H⁺-ATPase activity was similar between Col-0 and *vamp711*
307 mutant without ABA treatment (Figure 4E). After ABA treatment, the PM
308 H⁺-ATPase activity decreased in both the wild type and the *vamp711* mutant;
309 however, greater reduction was detected in the wild type than in the *vamp711*
310 mutant (Figure 4E). The immunoblot analysis showed that the PM H⁺-ATPase
311 protein levels were no different between Col-0 and *vamp711* mutants with or
312 without ABA treatment (Supplemental Figure S6A). These results together
313 suggested that ABA inhibits PM H⁺-ATPase activity at least partially through
314 VAMP711 interaction with the enzyme directly.

10



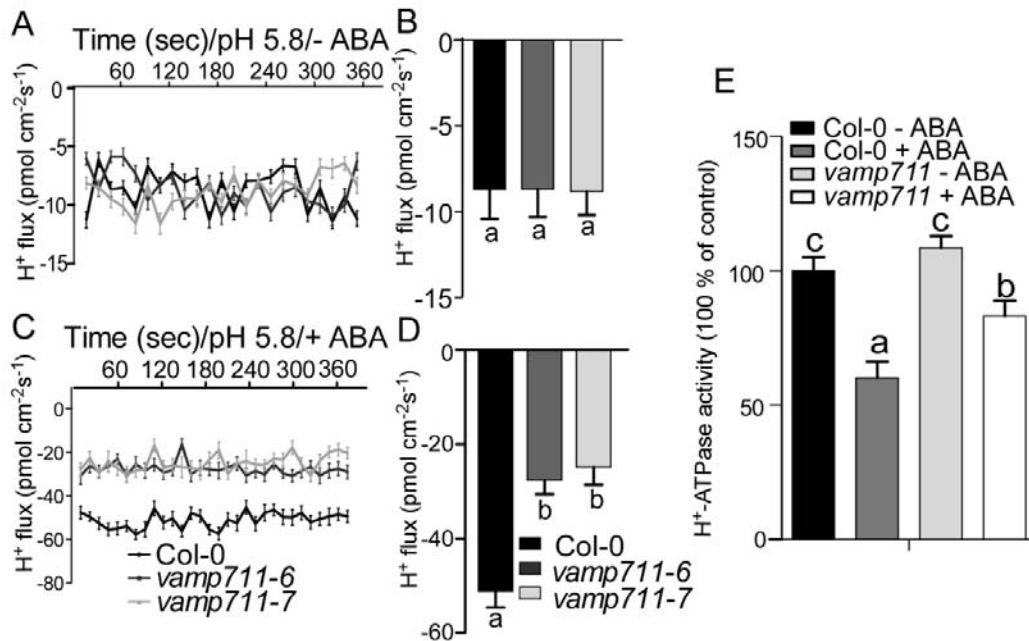
315

316 **VAMP711 inhibits AHA1-mediated stomatal closure and drought**
 317 **response**

318 Previous studies have shown that *vamp711* mutants are sensitive to drought
 319 stress and stomatal movement is impaired in the *vamp711* mutant (Leshem et
 320 al., 2010). Consistent with these findings, the water loss in *vamp711-6/7*
 321 mutants was more rapid than that in the wild type (Figures 5A and 5B); and
 322 both KCl-light-induced stomatal opening and ABA-induced stomatal closure
 323 were also impaired in *vamp711-6/7* mutants (Figure 5C).

324 The *ost2-2D* mutant contains two point mutations in the *AHA1* gene,
 325 resulting in AHA1 becoming constitutively hyperactive and the mutant
 326 becoming hypersensitive to drought stress (Merlot et al., 2007). To investigate
 327 whether the VAMP711-mediated plant ABA/drought response occurs through
 328 regulation of PM H⁺-ATPase activity, we crossed *OE-VAMP711-15* into the
 329 *ost2-2D* genetic background and obtained *ost2-2D-OE-VAMP711* plants. The
 330 Col-0, *ost2-2D*, *ost2-2D-OE-VAMP711* and *Col-0:OE-VAMP711* plants were
 331 grown in a greenhouse with 12 h light/12 h dark, and watering was stopped for
 332 5-week-old plants for 2 weeks. The wilting rate of the leaves in the *ost2-2D*
 333 mutant was much higher than that in other plants, and overexpression of
 334 VAMP711 in *ost2-2D* partially rescued its drought-sensitive phenotype (Figure
 335 6A), and the decreased chlorophyll and relative water contents in *ost2-2D*
 336 mutant were also partially rescued in *Col-0:OE-VAMP711* plants

11



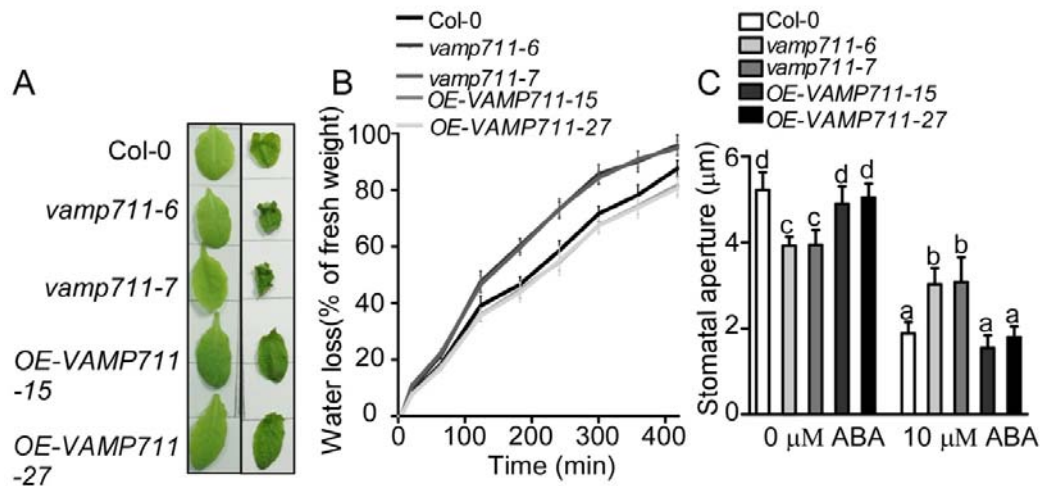
337 (Supplemental Figures S7A and S7B).

338 Consistent with this observation, the water loss of detached leaves in
 339 *ost2-2D-OE-VAMP711* was slower than that in *ost2-2D* and faster than that in
 340 *Col-0* and *Col-0:OE-VAMP711* (Figure 6B). In order to determine whether the
 341 overexpression of *VAMP711* represses ABA insensitivity of stomatal closure in
 342 *ost2-2D*, we performed the ABA-induced stomatal closure assay. Indeed,
 343 stomatal closure was insensitive to ABA in the *ost2-2D* mutant, and the
 344 overexpression of *VAMP711* partially rescued the *ost2-2D* stomatal closure
 345 phenotype in response to ABA (Figure 6C).

346 Since water loss by transpiration leads to temperature change in the leaf
 347 surface, we measured the leaf temperature of *Col-0*, *ost2-2D*,
 348 *ost2-2D-OE-VAMP711* and *OE-VAMP711* plants. The leaf temperature of
 349 *ost2-2D-OE-VAMP711* was higher than that of *ost2-2D* mutant (Figures 6D
 350 and 6E). We also transformed the *ProUBQ10:GFP-VAMP711* plasmid into the
 351 *ost2-2D* background and obtained two T₄ homologous lines,
 352 *ost2-2D-OE-VAMP711-1#1/2#*, in which the level of *VAMP711* expression was
 353 higher than that in *ost2-2D* (Supplemental Figure S7C). The
 354 *ost2-2D-OE-VAMP711-1/2#* displayed a phenotype similar to that of the
 355 *ost2-2D-OE-VAMP711* plants (Supplemental Figures S7E–S7F). Our results
 356 suggest that *VAMP711* interacts with and represses AHA1 activity.

357

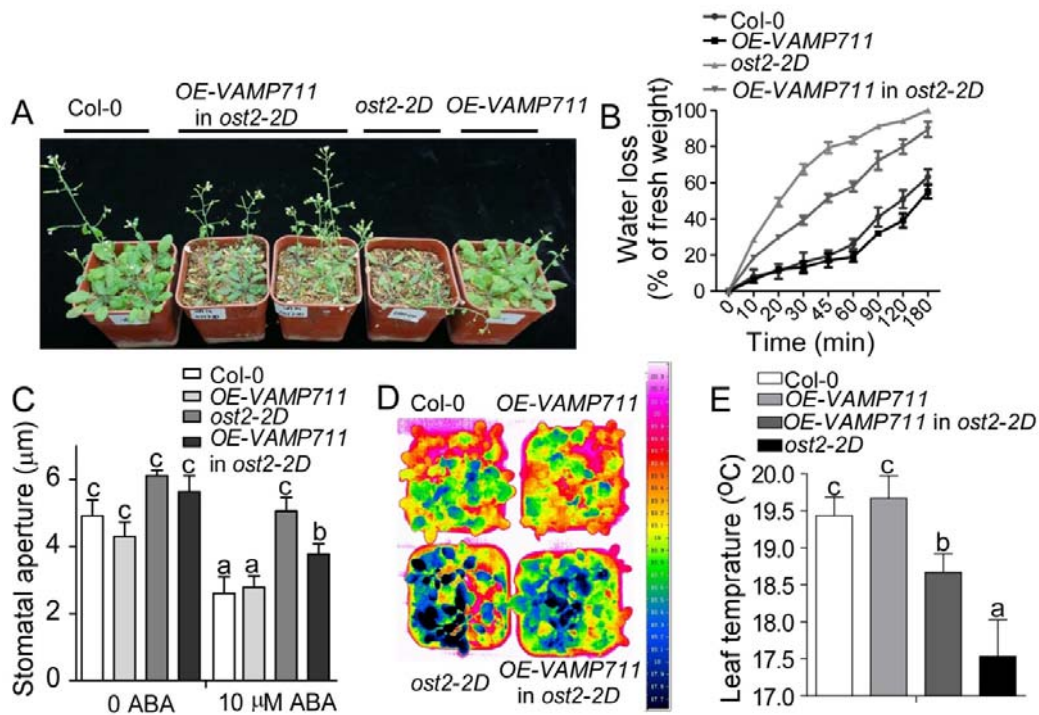
358



359 DISCUSSION

360 Drought is an adverse environmental factor that limits plant growth and crop
 361 productivity. Stomatal pores act as the gates for gas exchange (CO₂, O₂ and
 362 H₂O) and play an important role in the control of water loss in response to
 363 drought stress (Kim et al., 2010; Yamaguchi-Shinozaki and Shinozaki, 2006).
 364 Regulation of stomatal closure is the first step in response to water loss
 365 (Yamaguchi-Shinozaki and Shinozaki, 2006). Although a complex signal
 366 network regulates the process of stomatal closure, the only well-studied
 367 pathway is the ABA-mediated signaling pathway in drought stress response
 368 (Munemasa et al., 2015). The regulation of stomatal closure by ABA causes a
 369 series of physiological changes, such as cytoplasm alkalization, ion rebalance
 370 (Ca²⁺, K⁺), P-type H⁺-ATPase suppression (Fujii et al., 2009; Joshi-Saha et al.,
 371 2011; Pei et al., 1998). However, it is not well-understood how ABA-mediated
 372 PM H⁺-ATPase activity inhibition is regulated. In this study, we provide
 373 evidence that VAMP711 represses PM H⁺-ATPase activity to regulate
 374 ABA-dependent stomatal closure. Under drought stress, accumulation of ABA
 375 leads to VAMP711 physically interacting with AHA1 and AHA2 and inhibits
 376 their activities to promote stomatal closure (Figures 1B, 3A and 6C). VAMP711
 377 negatively regulates vacuolar H⁺-ATPase activity in yeast strains (Leshem et
 378 al., 2006), which suggests that VAMP711 may also play a role in regulating
 379 cytoplasm alkalization.

380 VAMP711 is highly expressed in guard cells in Arabidopsis, and
 381 down-regulation of *VAMP711* in Arabidopsis impairs stomatal closure during
 382 drought stress or ABA treatment (Leshem et al., 2010). However, the
 383 underlying mechanism is not clear. Our results demonstrate that VAMP711
 384 inhibits PM H⁺-ATPase activity through direct interaction to promote stomatal
 385 closure, indicating that VAMP711 and AHA1/AHA2 work together to regulate



386 stomatal closure in response to drought stress. VAMP711 protein is involved in
 387 endosome trafficking and vesicle fusion, and is reported to localize on the
 388 vacuolar membrane and PVC (Leshem et al., 2006); however, AHA1 and
 389 AHA2 are plasma membrane localized proteins (Harper et al., 1989). It is thus
 390 interesting to know the interacting location of these two proteins. The BiFC
 391 assay showed that the interaction between AHA1 and VAMP711 was on both
 392 the plasma membrane and punctate structures, indicating that VAMP711 could
 393 interact with AHA1 at least partially at the plasma membrane, although we
 394 could not exclude VAMP711 interaction with AHA1 in other locations.
 395 Intriguingly, studies with other proteins also showed similar phenomena. For
 396 example, catalase proteins localize in peroxisomes (Apel and Hirt, 2004);
 397 however, under salt and drought stresses, the plasma membrane proteins
 398 STRK1 (salt tolerance receptor-like cytoplasmic kinase 1, Zhou et al., 2018)
 399 and CPK8 (Calcium Protein Kinase 8, Zou et al., 2015) interact with,
 400 phosphorylate and activate CatC (in rice) and CAT3 (in Arabidopsis) on the
 401 plasma membrane, respectively. Therefore, it is possible that the VAMP711
 402 protein could be translocated to the plasma membrane through certain unclear
 403 mechanisms or under certain physiological conditions. Indeed, our results
 404 indicated that ABA treatment promoted the interaction of VAMP711 with AHA1
 405 and might partially affect the localization of VAMP711 to the plasma membrane.
 406 However, the observation and mechanism need to be further clarified. A recent
 407 study reported that VAMP711 is mislocalized to the plasma membrane in the
 408 *ap-3* mutant, providing a possibility for future study (Feng et al., 2017). In
 409 addition, other possibilities for the physical interaction between VAMP711 and
 410 AHA1 cannot be excluded. For example, it has been observed that PVC/MVB

411 could fuse with the plasma membrane during pathogen attack (An et al., 2006a;
412 An et al., 2006b). Thus, it is possible that PVCs with a small portion of
413 VAMP711 could move close to or fuse with the plasma membrane to promote
414 the interaction and inhibit PM H⁺-ATPase activity under drought stress (Vida
415 and Emr, 1995). This is supported by the fact that ABA treatment did not
416 dramatically induce the plasma membrane localization of VAMP711, as
417 determined by an immunoblot assay. Another possibility is the potential direct
418 membrane contact site (MCS) or stress-induced MCS between the tonoplast
419 and plasma membrane, which is yet to be observed (Perez-Sancho et al.,
420 2016). However, we also cannot exclude the possibility that VAMP711
421 represses PM H⁺-ATPase activity by regulating AHA1/AHA2 trafficking under
422 drought stress.

423 In Arabidopsis, AHA1 and AHA2 are two highly expressed proteins and
424 share higher similarity with other members of the AHA family. AHA1 and AHA2
425 are essential for plant growth and development, and the *aha1 aha2* double
426 mutant shows embryonic lethality (Harper et al., 1990). The AHA1 *ost2-2D*
427 mutant plants with constitutive higher PM H⁺-ATPase activity abolishes the
428 stomatal closure capacity under ABA treatment and are hypersensitive to
429 drought stress (Merlot et al., 2007), indicating that the repression of PM
430 H⁺-ATPase activity is essential for plant drought responses. SnRK2.2 but not
431 OST1/SnRK2.6 directly phosphorylates AHA2 *in vitro*, and the ABA-mediated
432 PM H⁺-ATPase activity inhibition is largely reduced in overexpression lines of
433 the protein phosphatase gene *HAB1*, *snrk2.2 snrk2.3* double mutant and ABA
434 sensors *pyr/pyl* sextuple mutant plants (Planes et al., 2015). OST1/SnRK2.6 is
435 required for the dephosphorylation of the Thr-947 site of AHA2 to inhibit PM
436 H⁺-ATPase activity (Merlot et al., 2007; Planes et al., 2015). These results
437 suggest that ABA signal is involved in inhibition of PM H⁺-ATPase activity in
438 response to drought stress. However, the detailed mechanism is not
439 understood.

440 In our study, we demonstrated that VAMP711 is involved in the
441 ABA-mediated inhibition of PM H⁺-ATPase activity. However, ABA treatment
442 also induced a decrease in PM H⁺-ATPase activity in the *vamp711* mutant,
443 although the decrease was not as great as in the wild type, suggesting that
444 VAMP711 functions redundantly with VAMP711 homologous proteins. In
445 Arabidopsis, the *VAMP7C* family contains four genes—*VAMP711-714*. It is
446 reported that they are all involved in regulating drought stress (Leshem et al.,
447 2010). It is possible that all VAMP7s are involved in the regulation of
448 ABA-mediated PM H⁺-ATPase activity inhibition.
449 Our results and previous reports show that overexpression of *VAMP711* does
450 not significantly improve plant drought resistance, suggesting that the
451 expression level of wild-type *VAMP711* is sufficient to regulate stomatal switch

452 in *Arabidopsis* (Leshem et al., 2010). In the *AHA1 ost2-2D* mutant, it required
453 more *VAMP711* molecules to bind more OST2-2D proteins to sufficiently inhibit
454 *AHA1* activity. On the other hand, other regulators, such as OST1/SnRK2.6,
455 SnRK2.2 and SnRK2.3, are required to regulate PM H⁺-ATPase activity in
456 response to drought stress.

457

458

459 **METHOD**

460 **Plant materials and growth**

461 The wild-type ecotype used in this study was *Arabidopsis thaliana* Col-0. The
462 mutant *ost2-2D* was described previously (Merlot et al., 2007). The
463 *AHA1*-overexpressing transgenic plants (*Pro*_{35S}:*GFP-AHA1*),
464 *VAMP711*-overexpressing transgenic plants (*Pro*_{UBQ10}:*GFP-VAMP711*) and the
465 complementary materials (*Pro*_{VAMP711}:*VAMP711*; com-1, 2) were generated
466 through *Agrobacterium strain* GV3101-mediated transformation. The
467 *VAMP711*-overexpressing transgenic plants in the *ost2-2D* mutant were
468 generated by crossing.

469 Seeds were sterilized in a solution containing 20% (v/v) sodium hypochlorite
470 and 0.1% (v/v) Triton X-100 for 10 min, washed five times with sterilized
471 distilled water and sown on Murashige and Skoog (MS) medium containing 2.5%
472 (w/v) sucrose and 0.3% (for horizontal growth) or 0.5% (for vertical growth)
473 Phytigel agar (Sigma-Aldrich), grown in a growth chamber at 23°C after
474 keeping them at 4°C for 3 days in darkness.

475 *Arabidopsis thaliana* and *Nicotiana benthamiana* plants were grown in soil
476 under 8 h light/16 h dark at 23°C and 60% relative humidity.

477

478 **Generation of *vamp711* CRISPR/Cas9 mutants**

479 A pair of selected sgRNA primers (C1: CCTCGTGGCTCGTGGCACGG and
480 C2: CGCCAAACAGATCCTCGAGA) in the *VAMP711* gene were cloned into
481 the *PHEC401* vector as described previously (Wang et al., 2015). The
482 construct was transformed into wild-type *Arabidopsis thaliana*. The
483 homozygous *vamp711* mutants (*vamp711-6*, *vamp711-7*) were identified by
484 sequencing.

485

486 **Split-Luciferase Complementation assays**

487 For the split-luciferase assays, the coding sequence of *VAMP711* was
488 amplified and cloned into *pCM1300-Cluc* and *pCM1300-Nluc* vectors between
489 the *KpnI* and *SalI* sites, respectively; and the coding sequence of *AHA1* was
490 also amplified and cloned into *pCM1300-Cluc* and *pCM1300-Nluc* vectors
491 between the *KpnI* and *SalI* sites, respectively. The constructs were
492 transformed into the *Agrobacterium strain* GV3101, and then infiltrated into *N.*
493 *benthamiana* leaves. LUC signal was collected after 3 days by using a cooled
494 charge-coupled device camera (ikon-L936; Andor Tech) after spraying 1 mM of
495 D-luciferin on the leaves (Promega) (Chen et al., 2008). Related LUC activity
496 was calculated using the Winvie32 software. Primer sequences are listed in
497 Supplemental Table 1.

498

499 **Bimolecular Fluorescence Complementation (BIFC) assay**

500 BIFC assay was used to detect the location of interaction between AHA1 and
501 VAMP711. The coding sequences of *AHA1* and *VAMP711* were cloned into
502 *pSYCE (MR)* and *pSYNE (R) 173* vectors at the *BamHI/SalI* and *SalI/KpnI*
503 sites, respectively. The coding sequence of *AHA1* was cloned into *pSYCE (MR)*
504 and *pSYNE (R) 173* vectors by using *BamHI/SalI*, respectively; the coding
505 sequence of *VAMP711* was also cloned into *pSYNE (R) 173* and *pSYCE (MR)*
506 vectors at the *SalI/KpnI* sites, respectively; and the coding sequence of *SYP22*
507 was cloned into *pSYCE (MR)* vector by using *BamHI/XhoI* (Waadt et al., 2008;
508 Walter et al., 2004). Primer sequences are listed in Supplemental Table 1. The
509 constructs were transformed into GV3101 and then infiltrated into *N.*
510 *benthamiana* leaves. The YFP fluorescence signal was detected using a Zeiss
511 LSM 710 META confocal microscope.

512

513 **Yeast Two-Hybrid assays**

514 The intracellular coding sequences of *AHA1*; *AHA1 (N)*, *AHA1 (centerloop)*,
515 *AHA1 (C100)*, *AHA1 (C100)^{Δ(887-897)}* and *AHA2 (C100)^{Δ(887-897)}* were cloned
516 into the *pGBKT7* vector between the *EcoRI* and *BamHI* sites. The C-terminus
517 coding sequences of *AHA3*, *AHA6* and *AHA9* were cloned into the *pGBKT7*
518 vector between the *EcoRI* and *BamHI* sites. The coding sequence of
519 *VAMP711*, which contains a longin domain and a SNARE domain, was cloned
520 into the *pGADT7* vector between the *EcoRI* and *BamHI* sites. Primer
521 sequences are listed in Supplemental Table 1. The indicated constructs were
522 transformed into the yeast strain AH109 and growth assays were based on
523 Yeast Protocols Handbook (Clontech).

524

525 **Reverse Transcription PCR (RT-PCR)**

526 Total RNA of 10-day-old seedlings grown on MS medium was extracted with
527 Trizol reagent (Invitrogen). RNase-free DNase I (Takara) was used to remove
528 genomic DNA in total RNA. Total RNA was reverse-transcribed with *Moloney*
529 *Murine Leukemia Virus* (MMLV) reverse transcriptase (Promega). The cDNA
530 was used for RT-PCR analysis.

531

532 **Confocal microscopy images**

533 Confocal images were captured using a Zeiss LSM 710 META confocal
534 microscope with a 40/1.4 oil objective. Five-day-old seedlings were stained
535 with 5 μM of FM4-64 (Invitrogen) for 1 or 5 min. GFP and FM4-64 fluorescent
536 signals were captured using multitrack function (488 nm for GFP, 561 nm for
537 Mcherry and FM4-64). Zeiss LSM image-processing software was used to

18

538 extract confocal images.

539 The PSC co-localization plug-in in the ImageJ program
540 (<http://rsb.info.nih.gov/ij/>) was used to analyze the co-localization of two
541 fluorescent signals. The values of the linear Pearson correlation coefficient
542 (RP) and nonlinear Spearman correlation coefficient (RS) were representative
543 for the extent of co-localization.

544

545 **Plasma membrane vesicles isolation**

546 Four-week-old plant materials were prepared for isolating plasma membrane
547 vesicles using the aqueous two-phase separation method (Qiu et al., 2002;
548 Yang et al., 2010). Plants were homogenized with an isolation buffer (0.33 M
549 sucrose, 0.2% (w/v) BSA, 10% (w/v) glycerol, 5 mM DTT, 5 mM EDTA, 5 mM
550 ascorbate, 0.6% (w/v) polyvinylpyrrolidone, and 0.2% (w/v) casein, 1 mM
551 PMSF and 50 mM HEPES-KOH, pH 7.5). The homogenate was centrifuged at
552 10,000 *g* for 10 min, and then the supernatant was filtered through two layers
553 of Miracloth. The microsomal pellet was obtained by centrifugation for 1 hour
554 at 100,000 *g* from the supernatant. The pellet was then resuspended in a
555 buffer I (0.33 M sucrose, 3 mM KCl, 1 mM DTT, 1 mM PMSF, 0.1 mM EDTA, 5
556 mM potassium phosphate and 1× protease inhibitor, pH 7.8). The prepared
557 two-phase mixture (6.2% (w/w) Dextran T-500, 0.33 M sucrose, 3 mM KCl and
558 6.2% (w/w) polyethylene glycol 3350 in 5 mM potassium phosphate, pH 7.8)
559 was used to separate the plasma membrane (up phase) from other
560 membranes (down phase). The final phases were collected and diluted with
561 buffer II (0.33 M sucrose, 10% (w/v) glycerol, 0.1% (w/v) BSA, 2 mM DTT, 0.1
562 mM EDTA, 20 mM HEPES-KOH and 1× protease inhibitor, pH 7.5), and then
563 centrifuged for 1 hour at 100,000 *g*. The pellet was resuspended with buffer I
564 containing 1 mM EDTA. Finally, the plasma membrane vesicles were used for
565 PM H⁺-ATPase activity and western blot analysis.

566

567 **PM H⁺-ATPase activity**

568 The H⁺-transport activity of PM H⁺-ATPase was measured as described
569 previously (Qiu et al., 2002). Transport of H⁺ by PM H⁺-ATPase forms an
570 inside-acid pH gradient (Δ pH) in the vesicles, and it was measured as a
571 decrease (quench) in the fluorescence of quinacrine (a pH-sensitive
572 fluorescence probe). The measurement buffer (2 mL) containing 5 mM
573 quinacrine, 3 mM MgSO₄, 100 mM KCl, and 25 mM 1, 3-Bis
574 [Tris(hydroxymethyl)methylamino] propane-HEPES, pH 6.5, 250 mM mannitol,
575 and 50 µg/mL of plasma membrane protein was used to detect the H⁺-ATPase
576 activity. The mixtures were incubated at 25°C in a cuvette and were placed in a

19

577 fluorescence spectrophotometer (Hitachi F-7000). Fluorescence reading was
578 begun when the mixtures were being stirred in dark for 5 min. H⁺-ATPase
579 activity was initiated by adding 3 mM of ATP, and the ΔpH was measured at
580 430 nm excitation and 500 nm emission wavelengths. To dissipate the
581 remaining pH gradient, 20 mM *m*-chlorophenylhydrazone (cccpc), a
582 protonophore, was added at the end of each reaction. The PM H⁺-ATPase
583 hydrolysis activity was measured as described previously (Qiu et al., 2002).

584

585 **Mensuration of H⁺ flux**

586 The H⁺ fluxes were measured in the meristematic zone (approximately 100 μm
587 from the root tip) using the non-invasive micro-test technique (NMT; Younger
588 USA LLC, Amherst, MA, USA; Xuyue (Beijing) Sci & Tech Co., Ltd, Beijing,
589 China) (Yang et al., 2010). The H⁺ selective micropipettes were filled with
590 10-μm columns of H⁺-selective liquid exchange cocktails (LIXs) (Fluka 95293).
591 An Ag/AgCl wire electrode was inserted into the micropipettes from the back
592 such that it made contact with the electrolyte buffer. The H⁺ concentration was
593 evaluated by moving the H⁺ microelectrode between two positions at 20–40
594 μm from the root. Five-day-old Arabidopsis seedlings were treated with a
595 pH-7.8 buffer (0.1 mM CaCl₂, 0.1 mM KCl, 0.03 mM HEPS and 75 mM NaCl)
596 and a pH-5.8 buffer (0.1 mM CaCl₂, 0.1 mM KCl, 0.03 mM MES). To detect the
597 effect of ABA on H⁺ flux, 2 μM of ABA was added into above-mentioned buffer.

598

599 **Water loss and stomatal aperture assays**

600 The rosette leaves from 5-week-old plants in soil were detached to examine
601 water loss, and the photographs of leaves were taken after 0 and 3 hours after
602 detachment. To measure the rate of water loss, the 5-week-old plants in soil
603 were used to perform water loss measurement. The weight of the detached
604 leaves was measured every 0.5 hour.

605 The rosette leaves of 5-week-old plants in soil were used to detect the
606 stomatal closure under the ABA treatment. The leaves were incubated in
607 opening buffer (50 mM KCl, 10 mM CaCl₂, and 10 mM MES, pH 6.15) in a
608 growth chamber for 2 hours to open stomatal pores completely. Stomatal
609 apertures were measured after adding 10 of mM ABA for 2 hours. More than
610 70 stomatal pores were observed to measure the aperture in three
611 independent experiments.

612

613 **Chlorophyll content analysis**

614 The rosette leaves from 5-week-old plants in soil with 12 h light/12 h dark were
615 used to determine chlorophyll content. The rosette leaves were weighed and

20

616 added in 1 mL of 80% (v/v) acetone, and then the samples were incubated in
617 darkness for 12 hours at room temperature. The absorption of each sample
618 was measured at 663 and 645 nm with a spectrophotometer. The chlorophyll
619 content was calculated as follows: total chlorophyll = Chla + Chlb.

620

621 **Relative water content**

622 The 5-week-old plants in soil with 12 h light/12 h dark were used to detect
623 relative water content. The fresh weight (W_{fresh}) was determined, and then the
624 samples were dried at 65°C for 2 days and weighed to determine the dry
625 weight (W_{dry}). The relative water content was calculated as follows: relative
626 water content (%) = $(W_{\text{fresh}} - W_{\text{dry}}) / W_{\text{fresh}} * 100\%$.

627

628 **Infrared Thermograph Imaging**

629 Thermal imaging was used to monitor the leaf temperature as described
630 previously (Xie et al., 2006). The plants were well watered, and watering was
631 stopped for 1 week to decrease plant humidity. Five-week-old plants in soil
632 were used to measure leaf temperature by thermal imaging camera.

633

634 **Accession Numbers**

635 Sequence data in this study can be found in the Arabidopsis Genome Initiative
636 database under the following accession numbers: *VAMP711*, *At4g32150*;
637 *AHA1*, *At2g18960*; *AHA2*, *At4g30190*.

638

639 **Supplemental Data**

640

641 The following supplemental materials are available.

642

643 **Supplemental Figure S1.** Effect of ABA on PM H⁺-ATPase activity in
644 Arabidopsis

645 **Supplemental Figure S2.** Analysis of the localization of and the interaction
646 between AHA1 and VAMP711

647 **Supplemental Figure S3.** VAMP711 interacts with the C-terminus of AHA2

648 **Supplemental Figure S4.** The *vamp711* mutants are generated by
649 CRISPR/Cas9 technology

650 **Supplemental Figure S5.** The *vamp711* mutants are tolerant to high pH

651 **Supplemental Figure S6.** The analysis of PM H⁺-ATPase protein level in the
652 plasma membrane in Col-0 and *vamp711* mutant seedlings

653 **Supplemental Figure S7.** The drought-stress phenotype and expression level
654 of *VAMP711* in the indicated plants

655

656 **Supplemental Table 1** Primers used in this study

657

658 **ACKNOWLEDGEMENTS**

659 This work was supported by the National Genetically Modified Organisms
660 Breeding Major Projects (2016ZX08009002), National Natural Science
661 Foundation of China (31430012, U1706201, 31670260).

662

663 **Figure Legends**

664

665 **Figure 1 VAMP711 interacts with PM H⁺-ATPase AHA1**

666

667 A. Luciferase complementation assay. The indicated constructs were
668 expressed in *Nicotiana benthamiana* leaves. 1: *AHA1^{Nluc}* and *^{Cluc}DDM1*; 2-3:
669 *AHA1^{Nluc}* and *^{Cluc}VAMP711*; 4: *DDM1^{Nluc}* and *^{Cluc}VAMP711*. The luciferase
670 signal was detected using a cooled charge-coupled device camera (ikon-L936;
671 Andor Tech).

672 B. ABA induced the interaction between AHA1 and VAMP711. *AHA1^{Nluc}* and
673 *^{Cluc}VAMP711* were transformed into *N. benthamiana* leaves. After a 3-day
674 incubation, the leaves were treated with or without ABA. The luciferase value
675 was collected using a spectrophotometer. Error bars represent SD (small
676 leaves acquired by a leaf punch, number, 10); Student's *t* test was used to
677 assess statistical significance ($p \leq 0.05$).

678

679 **Figure 2 VAMP711 interacts with the C-terminus of AHA1 and AHA2**

680

681 A. Schematic structure of *VAMP711* protein structure: longin domain, SNARE
682 domain and transmembrane domain (TMD). The longin and SNARE domains
683 of *VAMP711* (*VAMP711*-LS) were used in a yeast two-hybrid assay.

684 B. Yeast two-hybrid assay to detect the interaction between the AHA1
685 N-terminus, centerloop, C-terminus and *VAMP711*.

686 C. The sequence alignment analysis of the C-terminus of PM H⁺-ATPase (AHA)
687 in Arabidopsis.

688 D. Yeast two-hybrid assay to detect the interaction of *VAMP711* with the
689 C-terminus of AHA family members.

690 E. Yeast two-hybrid assay to detect the region of interaction between AHA1
691 C-terminus, AHA1 C-terminus minus amino acid residues 887 to 897 (*AHA1*
692 (*C100*) ^{Δ 887-897}) and *VAMP711*.

693 Yeast strains expressing the indicated plasmids were grown on synthetic
694 complete medium without Trp and Leu (SC-WL, left panel) and on synthetic

22

695 complete medium without Trp, Leu and His (SC-WHL, right panel).
696 Photographs were taken after 3 to 5 days of growth on the indicated medium.
697 Panels show yeast serial decimal dilutions. Experimental details are provided
698 in Methods.

699

700 **Figure 3 VAMP711 negatively regulates PM H⁺-ATPase activity**

701

702 A. PM H⁺-ATPase activity was measured in Col-0, *vamp711-6*, *vamp711-7* and
703 *OE-VAMP711-15/27*. Plasma membrane vesicles of Col-0, *vamp711-6*,
704 *vamp711-7*, *OE-VAMP711-15/27* were isolated from 4-week-old soil-grown
705 plants treated with 200 mM of NaHCO₃ for 3 days. Error bars represent SD;
706 Student's *t* test was used to assess statistical significance ($p \leq 0.05$). The
707 experiment was repeated three times independently.

708 B. Comparison of PM H⁺-ATPase activity from (A).

709 C. Net H⁺ fluxes in different plant materials. Five-day-old seedlings of Col-0,
710 *vamp711-6*, *vamp711-7*, *OE-VAMP711-15/27* were treated with a buffer (0.5
711 mM KCl, 0.1 mM CaCl₂, 75 mM NaCl and 0.03 mM HEPS, pH 7.8) for 30 min,
712 and then the H⁺ fluxes in the root tips was detected by the non-invasive
713 micro-test technique. Error bars represent SD (seedling number ≥ 10);
714 Student's *t* test was used to assess statistical significance ($p \leq 0.05$).

715 Experiment was repeated three times independently.

716 D. Calculated net H⁺ fluxes from (C).

717 E. VAMP711 inhibits PM H⁺-ATPase activity *in vitro*. Fifty nanograms of
718 plasma membrane vesicles from Col-0 was incubated with 500 ng of
719 VAMP711-LS protein for 15 min at room temperature. The experiment is
720 described in Methods and repeated three times independently.

721 F. Comparison of PM H⁺-ATPase activity from (E).

722 G. VAMP711 inhibits the PM H⁺-ATPase activity of AHA2 in the RS72 yeast
723 strain. VAMP711 and an empty vector were transferred into the RS72 yeast
724 strain containing AHA2. The endogenous H⁺-ATPase gene in RS72 was
725 induced by galactose (gal). When AHA2 and VAMP711 were transferred into
726 the RS72 yeast strain, the growth of the yeast depended on AHA2 activity on
727 glucose (glu) medium. Photographs were taken after 3 to 5 days of growth on
728 the indicated medium. Panels show yeast serial half dilutions. Experimental
729 details are provided in Methods. The experiment was repeated at least three
730 times independently.

731

732 **Figure 4 VAMP711 is involved in ABA-mediated inhibition of PM**
733 **H⁺-ATPase activity**

734

735 A. Net H⁺ fluxes in root tips of Col-0, *vamp711-6* and *vamp711-7*. Five-day-old
736 seedlings were treated with a buffer (0.5 mM KCl, 0.1 mM CaCl₂, and 0.03 mM
737 MES, pH 5.8) for 30 min, and then the H⁺ flux was detected in root tips. Error
738 bars represent SD (seedling number ≥ 10); Student's *t* test was used to assess
739 statistical significance (p≤0.05). The experiment was repeated three times
740 independently.

741 B. Net H⁺ fluxes calculated from (A).

742 C. Net H⁺ fluxes in the root tips in the presence of ABA. Five-day-old seedlings
743 of Col-0, *vamp711-6* and *vamp711-7* were treated with a buffer (0.5 mM KCl,
744 0.1 mM CaCl₂, and 0.03 mM MES, 2 μM ABA, pH 5.8) for 30 min, and the H⁺
745 fluxes were detected in the root tips. Error bars represent SD (seedling number
746 ≥ 10); Student's *t* test was used to assess statistical significance (p≤0.05). The
747 experiment was repeated three times independently.

748 D. Net H⁺ fluxes calculated from (C).

749 E. PM H⁺-ATPase activity was measured in Col-0 and *vamp711-6* with or
750 without ABA treatment. Plasma membrane vesicles of Col-0, *vamp711-6* were
751 isolated from 4-week-old plants treated with 10 μM of ABA for 1 day. Error bars
752 represent SD; Student's *t* test was used to assess statistical significance
753 (p≤0.05). The experiment was repeated three times independently.

754

755 **Figure 5 VAMP711 is involved in drought stress response**

756

757 A. Detached rosette leaves from Col-0, *vamp711-6*, *vamp711-7* and
758 *OE-VAMP711-15/27*. Photographs were taken at 0 (left) and 3 hours (right).

759 B. Water-loss measurement of detached leaves. Col-0, *vamp711-6*,
760 *vamp711-7* and *OE-VAMP711-15/27* were grown in short-day conditions for 5
761 weeks. Fresh weight of detached leaves was monitored at the indicated times.
762 The experiment was repeated three times independently.

763 C. Stomatal aperture assay. Detached rosette leaves from Col-0, *vamp711-6*
764 and *vamp711-7* were incubated in KCl buffer for about 2 hours and then
765 transferred in a buffer containing 10 μM of ABA for 2 hours. Error bars
766 represent SD (stomata number, 70); Student's *t* test was used to assess
767 statistical significance (p≤0.05). The experiment was repeated three times
768 independently.

769

770 **Figure 6 VAMP711 regulates AHA1-mediated stomatal closure**

771

772 A. Drought phenotype of the Col-0, *ost2-2D*, *OE-VAMP711* in *ost2-2D* and

24

773 *OE-VAMP711* grown in soil. Watering was stopped for five-week-old plants
774 grown in soil under 12 h light/12 h dark for 2 weeks, and then photographs
775 were taken.

776 B. Measurement of water loss from detached leaves. Col-0, *ost2-2D*,
777 *OE-VAMP711* in *ost2-2D* and *OE-VAMP711* were grown under short-day
778 conditions for 5 weeks, and the fresh weight of detached seedlings was
779 monitored at the indicated times. The experiment was repeated three times
780 independently.

781 C. ABA induced stomatal closure assay. Detached rosette leaves from Col-0,
782 *ost2-2D*, *OE-VAMP711* in *ost2-2D* and *OE-VAMP711* were incubated in KCl
783 buffer for about 2 hours and then transferred in a buffer containing 10 μ M of
784 ABA for 2 hours. Error bars represent SD (stomata number, 70); Student's *t*
785 test was used to assess statistical significance ($p \leq 0.05$). The experiment was
786 repeated three times independently.

787 D. Pseudo-color infrared images of Col-0, *ost2-2D*, *OE-VAMP711* in *ost2-2D*
788 and *OE-VAMP711*. The images of 5-week-old plants in soil were taken using an
789 infrared camera.

790 E. Leaf temperature measurement from (D) using infrared camera software.
791 Error bars represent SD (20 leaves were used), Student's *t* test was used to
792 assess statistical significance ($p \leq 0.05$).



Parsed Citations

An, Q., Ehlers, K., Kogel, K.H., Bel, A.J.E.V., and Hükelhoven, R. (2006a). Multivesicular compartments proliferate in susceptible and resistant MLA12- barley leaves in response to infection by the biotrophic powdery mildew fungus. *New Phytol* 172: 563-576.

Pubmed: [Author and Title](#)

Google Scholar: [Author Only Title Only Author and Title](#)

An, Q., Huckelhoven, R., Kogel, K.H., and van Bel, A.J. (2006b). Multivesicular bodies participate in a cell wall-associated defence response in barley leaves attacked by the pathogenic powdery mildew fungus. *Cell Microbiol* 8: 1009-1019.

Pubmed: [Author and Title](#)

Google Scholar: [Author Only Title Only Author and Title](#)

Apel, K., and Hirt, H. (2004). Reactive oxygen species: metabolism, oxidative stress, and signal transduction. *Annu Rev Plant Biol* 55: 373-399.

Pubmed: [Author and Title](#)

Google Scholar: [Author Only Title Only Author and Title](#)

Basu, J., Shen, N., Dulubova, I., Lu, J., Guan, R., Guryev, O., Grishin, N.V., Rosenmund, C., and Rizo, J. (2005). A minimal domain responsible for Munc13 activity. *Nat Struct Mol Biol* 12: 1017-1018.

Pubmed: [Author and Title](#)

Google Scholar: [Author Only Title Only Author and Title](#)

Cai, S., Chen, G., Wang, Y., Huang, Y., Marchant, D.B., Wang, Y., Yang, Q., Dai, F., Hills, A., Franks, P.J., et al. (2017). Evolutionary conservation of ABA signaling for stomatal closure. *Plant Physiol* 174: 732-747.

Pubmed: [Author and Title](#)

Google Scholar: [Author Only Title Only Author and Title](#)

Camoni, L., Iori, V., Marra, M., and Aducci, P. (2000). Phosphorylation-dependent interaction between plant plasma membrane H⁺-ATPase and 14-3-3 proteins. *J Biol Chem* 275: 9919-9923.

Pubmed: [Author and Title](#)

Google Scholar: [Author Only Title Only Author and Title](#)

Chen, H., Zou, Y., Shang, Y., Lin, H., Wang, Y., Cai, R., Tang, X., and Zhou, J.M. (2008). Firefly Luciferase Complementation imaging assay for Protein-Protein interactions in plants. *Plant Physiol* 146: 368.

Pubmed: [Author and Title](#)

Google Scholar: [Author Only Title Only Author and Title](#)

Collins, N.C., Thordal-Christensen, H., Lipka, V., Bau, S., Kombrink, E., Qiu, J.L., Huckelhoven, R., Stein, M., Freialdenhoven, A., Somerville, S.C., et al. (2003). SNARE-protein-mediated disease resistance at the plant cell wall. *Nature* 425: 973-977.

Pubmed: [Author and Title](#)

Google Scholar: [Author Only Title Only Author and Title](#)

Falhof, J., Pedersen, J.T., Fuglsang, A.T., and Palmgren, M. (2016). Plasma membrane H⁺-ATPase regulation in the center of plant physiology. *Mol Plant* 9: 323-337.

Pubmed: [Author and Title](#)

Google Scholar: [Author Only Title Only Author and Title](#)

Feng, Q.N., Song, S.J., Yu, S.X., Wang, J.G., Li, S., and Zhang, Y. (2017). Adaptor Protein-3-Dependent vacuolar trafficking involves a subpopulation of COPII and HOPS tethering proteins. *Plant Physiol* 174: 1609-1620.

Pubmed: [Author and Title](#)

Google Scholar: [Author Only Title Only Author and Title](#)

Fuglsang, A.T., Guo, Y., Cui, T.A., Qiu, Q., Song, C., Kristiansen, K.A., Bych, K., Schulz, A., Shabala, S., Schumaker, K.S., et al. (2007). Arabidopsis protein kinase PKS5 inhibits the plasma membrane H⁺-ATPase by preventing interaction with 14-3-3 protein. *Plant Cell* 19: 1617-1634.

Pubmed: [Author and Title](#)

Google Scholar: [Author Only Title Only Author and Title](#)

Fujii, H., Chinnusamy, V., Rodrigues, A., Rubio, S., Antoni, R., Park, S.Y., Cutler, S.R., Sheen, J., Rodriguez, P.L., and Zhu, J.K. (2009). In vitro reconstitution of an abscisic acid signalling pathway. *Nature* 462: 660-664.

Pubmed: [Author and Title](#)

Google Scholar: [Author Only Title Only Author and Title](#)

Fujiwara, M., Uemura, T., Ebine, K., Nishimori, Y., Ueda, T., Nakano, A., Sato, M.H., and Fukao, Y. (2014). Interactomics of Qa-SNARE in *Arabidopsis thaliana*. *Plant & Cell Physiol* 55: 781-789.

Pubmed: [Author and Title](#)

Google Scholar: [Author Only Title Only Author and Title](#)

Gévaudant, F., Duby, G., Von, S.E., Zhao, R., Morsomme, P., and Boutry, M. (2007). Expression of a constitutively activated plasma membrane H⁺-ATPase alters plant development and increases salt tolerance. *Plant Physiol* 144: 1763.

Pubmed: [Author and Title](#)

Google Scholar: [Author Only Title Only Author and Title](#)

Harper, J.F., Manney, L., DeWitt, N.D., Yao, M.H., and Sussman, M.R. (1990). The *Arabidopsis thaliana* plasma membrane H⁺-ATPase

multigene family. Genomic sequence and expression of a third isoform. J Biol Chem 265: 13601-13608.

Pubmed: [Author and Title](#)

Google Scholar: [Author Only Title Only Author and Title](#)

Harper, J.F., Surowy, T.K., and Sussman, M.R. (1989). Molecular cloning and sequence of cDNA encoding the plasma membrane proton pump (H⁺-ATPase) of Arabidopsis thaliana. Proc Natl Acad Sci USA 86: 1234-1238.

Pubmed: [Author and Title](#)

Google Scholar: [Author Only Title Only Author and Title](#)

Haruta, M., Tan, L.X., Bushey, D.B., Swanson, S.J., and Sussman, M.R. (2017). Environmental and genetic factors regulating localization of the plant plasma membrane H⁺-ATPase. Plant Physiol 176: 364-377.

Pubmed: [Author and Title](#)

Google Scholar: [Author Only Title Only Author and Title](#)

Hashimoto-Sugimoto, M., Higaki, T., Yaeno, T., Nagami, A., Irie, M., Fujimi, M., Miyamoto, M., Akita, K., Negi, J., Shirasu, K., et al. (2013). A Munc13-like protein in Arabidopsis mediates H⁺-ATPase translocation that is essential for stomatal responses. Nat Commun 4: 2215.

Pubmed: [Author and Title](#)

Google Scholar: [Author Only Title Only Author and Title](#)

Hong, W. (2005). SNAREs and traffic. Biochim Biophys Acta 1744: 493-517.

Pubmed: [Author and Title](#)

Google Scholar: [Author Only Title Only Author and Title](#)

Jahn, R., and Scheller, R.H. (2006). SNAREs-engines for membrane fusion. Nat Rev Mol Cell Bio 7: 631-643.

Pubmed: [Author and Title](#)

Google Scholar: [Author Only Title Only Author and Title](#)

Joshi-Saha, A., Valon, C., and Leung, J. (2011). Abscisic acid signal off the starting block. Mol Plant 4: 562-580.

Pubmed: [Author and Title](#)

Google Scholar: [Author Only Title Only Author and Title](#)

Kim, T.H., Bohmer, M., Hu, H., Nishimura, N., and Schroeder, J.I. (2010). Guard cell signal transduction network: advances in understanding abscisic acid, CO₂, and Ca²⁺ signaling. Annu Rev Plant Biol 61: 561-591.

Pubmed: [Author and Title](#)

Google Scholar: [Author Only Title Only Author and Title](#)

Kinoshita, T., and Shimazaki, K. (2002). Biochemical evidence for the requirement of 14-3-3 protein binding in activation of the guard-cell plasma membrane H⁺-ATPase by blue light. Plant & Cell Physiol 43: 1359-1365.

Pubmed: [Author and Title](#)

Google Scholar: [Author Only Title Only Author and Title](#)

Leshem, Y., Golani, Y., Kaye, Y., and Levine, A. (2010). Reduced expression of the v-SNAREs AtVAMP71/AtVAMP7C gene family in Arabidopsis reduces drought tolerance by suppression of abscisic acid-dependent stomatal closure. J Exp Bot 61: 2615-2622.

Pubmed: [Author and Title](#)

Google Scholar: [Author Only Title Only Author and Title](#)

Leshem, Y., Melamed-Book, N., Cagnac, O., Ronen, G., Nishri, Y., Solomon, M., Cohen, G., and Levine, A. (2006). Suppression of Arabidopsis vesicle-SNARE expression inhibited fusion of H₂O₂-containing vesicles with tonoplast and increased salt tolerance. P Natl Acad Sci USA 103: 18008-18013.

Pubmed: [Author and Title](#)

Google Scholar: [Author Only Title Only Author and Title](#)

Merlot, S., Leonhardt, N., Fenzi, F., Valon, C., Costa, M., Piette, L., Vavasseur, A., Genty, B., Boivin, K., Muller, A., et al. (2007). Constitutive activation of a plasma membrane H⁺-ATPase prevents abscisic acid-mediated stomatal closure. The EMBO J 26: 3216-3226.

Pubmed: [Author and Title](#)

Google Scholar: [Author Only Title Only Author and Title](#)

Munemasa, S., Hauser, F., Park, J., Waadt, R., Brandt, B., and Schroeder, J.I. (2015). Mechanisms of abscisic acid-mediated control of stomatal aperture. Curr Opin Plant Biol 28: 154-162.

Pubmed: [Author and Title](#)

Google Scholar: [Author Only Title Only Author and Title](#)

Palmgren, M.G. (2001). Plant plasma membrane H⁺-ATPases: powerhouses for nutrient uptake. Annu Rev Plant Physiol Mol Biol 52: 817-845.

Pubmed: [Author and Title](#)

Google Scholar: [Author Only Title Only Author and Title](#)

Palmgren, M.G., Sommarin, M., Serrano, R., and Larsson, C. (1991). Identification of an autoinhibitory domain in the C-terminal region of the plant plasma membrane H⁺-ATPase. J Biol Chem 266: 20470-20475.

Pubmed: [Author and Title](#)

Google Scholar: [Author Only Title Only Author and Title](#)

Pei, Z.M., Ghassemian, M., Kwak, C.M., McCourt, P., and Schroeder, J.I. (1998). Role of farnesyltransferase in ABA regulation of guard cell anion channels and plant water loss. Science 282: 287-290.

Pubmed: [Author and Title](#)
Google Scholar: [Author Only Title Only Author and Title](#)

Perez-Sancho, J., Tilsner, J., Samuels, A.L., Botella, M.A., Bayer, E.M., and Rosado, A. (2016). Stitching organelles: organization and function of specialized membrane contact sites in plants. Trends cell biol 26: 705-717.

Pubmed: [Author and Title](#)
Google Scholar: [Author Only Title Only Author and Title](#)

Planes, M.D., Ninoles, R., Rubio, L., Bissoli, G., Bueso, E., Garcia-Sanchez, M.J., Alejandro, S., Gonzalez-Guzman, M., Hedrich, R., Rodriguez, P.L., et al. (2015). A mechanism of growth inhibition by abscisic acid in germinating seeds of *Arabidopsis thaliana* based on inhibition of plasma membrane H⁺-ATPase and decreased cytosolic pH, K⁺, and anions. J Exp Bot 66: 813-825.

Pubmed: [Author and Title](#)
Google Scholar: [Author Only Title Only Author and Title](#)

Pratelli, R., Sutter, J.U., and Blatt, M.R. (2004). A new catch in the SNARE. Trends Plant Sci 9: 187-195.

Pubmed: [Author and Title](#)
Google Scholar: [Author Only Title Only Author and Title](#)

Qiu, Q.S., Y, G., MA, D., KS, S., and JK, Z. (2002). Regulation of SOS1, a plasma membrane Na⁺/H⁺ exchanger in *Arabidopsis thaliana*, by SOS2 and SOS3. P Natl Acad Sci USA 99: 8436.

Pubmed: [Author and Title](#)
Google Scholar: [Author Only Title Only Author and Title](#)

Roberkleber, N., Albrechtová, J.T.P., Fleig, S., Huck, N., Michalke, W., Wagner, E., Speth, V., Neuhaus, G., and Fischeriglesias, C. (2003). Plasma membrane H⁺-ATPase is involved in Auxin-Mediated cell elongation during wheat embryo development. Plant Physiol 131: 1302-1312.

Pubmed: [Author and Title](#)
Google Scholar: [Author Only Title Only Author and Title](#)

Sanderfoot, A. (2007). Increases in the number of SNARE genes parallels the rise of multicellularity among the green plants. Plant Physiol 144: 6-17.

Pubmed: [Author and Title](#)
Google Scholar: [Author Only Title Only Author and Title](#)

Sugano, S., Hayashi, N., Kawagoe, Y., Mochizuki, S., Inoue, H., Mori, M., Nishizawa, Y., Jiang, C.J., Matsui, M., and Takatsuji, H. (2016). Rice OsVAMP714, a membrane-trafficking protein localized to the chloroplast and vacuolar membrane, is involved in resistance to rice blast disease. Plant Mol Biol 91: 81-95.

Pubmed: [Author and Title](#)
Google Scholar: [Author Only Title Only Author and Title](#)

Svennelid, F., Olsson, A., Piotrowski, M., Rosenquist, M., Ottman, C., Larsson, C., Oecking, C., and Sommarin, M. (1999). Phosphorylation of Thr-948 at the C terminus of the plasma membrane H⁺-ATPase creates a binding site for the regulatory 14-3-3 protein. Plant Cell 11: 2379-2391.

Pubmed: [Author and Title](#)
Google Scholar: [Author Only Title Only Author and Title](#)

Uemura, T., Sato, M.H., and Takeyasu, K. (2005). The longin domain regulates subcellular targeting of VAMP7 in *Arabidopsis thaliana*. FEBS Lett 579: 2842-2846.

Pubmed: [Author and Title](#)
Google Scholar: [Author Only Title Only Author and Title](#)

Uemura, T., Ueda, T., Ohniwa, R.L., Nakano, A., Takeyasu, K., and Sato, M.H. (2004). Systematic analysis of SNARE molecules in *Arabidopsis*: dissection of the post-Golgi network in plant cells. Cell Struct Funct 29: 49-65.

Pubmed: [Author and Title](#)
Google Scholar: [Author Only Title Only Author and Title](#)

Vida, T.A., and Emr, S.D. (1995). A new vital stain for visualizing vacuolar membrane dynamics and endocytosis in yeast. J Cell Biol 128: 779-792.

Pubmed: [Author and Title](#)
Google Scholar: [Author Only Title Only Author and Title](#)

Waadt, R., Schmidt, L.K., Lohse, M., Hashimoto, K., and Bock, R. (2008). Multicolor bimolecular fluorescence complementation reveals simultaneous formation of alternative CBL/CIPK complexes in planta. Plant J 56: 505.

Pubmed: [Author and Title](#)
Google Scholar: [Author Only Title Only Author and Title](#)

Walter, M., Chaban, C., Schütze, K., Batistic, O., Weckermann, K., Näke, C., Blazevic, D., Grefen, C., Schumacher, K., and Oecking, C. (2004). Visualization of protein interactions in living plant cells using bimolecular fluorescence complementation. Plant J 40: 428.

Pubmed: [Author and Title](#)
Google Scholar: [Author Only Title Only Author and Title](#)

Wang, Z.P., Xing, H.L., Dong, L., Zhang, H.Y., Han, C.Y., Wang, X.C., and Chen, Q.J. (2015). Egg cell-specific promoter-controlled CRISPR/Cas9 efficiently generates homozygous mutants for multiple target genes in *Arabidopsis* in a single generation. Genome Bio 16: 144.

Pubmed: [Author and Title](#)

Google Scholar: [Author Only Title Only Author and Title](#)

Xie, X., Wang, Y., Williamson, L., Holroyd, G.H., Tagliavia, C., Murchie, E., Theobald, J., Knight, M.R., Davies, W.J., and Leyser, H.M.O. (2006). The identification of genes involved in the stomatal response to reduced atmospheric relative humidity. *Curr Biol* 16: 882-887.

Pubmed: [Author and Title](#)

Google Scholar: [Author Only Title Only Author and Title](#)

Yamaguchi-Shinozaki, K., and Shinozaki, K. (2006). Transcriptional regulatory networks in cellular responses and tolerance to dehydration and cold stresses. *Ann Rev Plant Biol* 57: 781-803.

Pubmed: [Author and Title](#)

Google Scholar: [Author Only Title Only Author and Title](#)

Yamauchi, S., Takemiya, A., Sakamoto, T., Kurata, T., Tsutsumi, T., Kinoshita, T., and Shimazaki, K. (2016). The plasma membrane H⁺-ATPase AHA1 plays a major role in stomatal opening in response to blue light. *Plant Physiol* 171: 2731-2743.

Pubmed: [Author and Title](#)

Google Scholar: [Author Only Title Only Author and Title](#)

Yang, Y., Qin, Y., Xie, C., Zhao, F., Zhao, J., Liu, D., Chen, S., Fuglsang, A.T., Palmgren, M.G., Schumaker, K.S., et al. (2010). The Arabidopsis chaperone J3 regulates the plasma membrane H⁺-ATPase through interaction with the PKS5 kinase. *Plant Cell* 22: 1313-1332.

Pubmed: [Author and Title](#)

Google Scholar: [Author Only Title Only Author and Title](#)

Yin, Y., Adachi, Y., Ye, W., Hayashi, M., Nakamura, Y., Kinoshita, T., Mori, I.C., and Murata, Y. (2013). Difference in abscisic acid perception mechanisms between closure induction and opening inhibition of stomata. *Plant Physiol* 163: 600-610.

Pubmed: [Author and Title](#)

Google Scholar: [Author Only Title Only Author and Title](#)

Zhang, B., Karnik, R., Wang, Y., Wallmeroth, N., Blatt, M.R., and Grefen, C. (2015). The Arabidopsis R-SNARE VAMP721 interacts with KAT1 and KC1 K⁺ channels to moderate K⁺ current at the plasma membrane. *Plant Cell* 27: 1697-1717.

Pubmed: [Author and Title](#)

Google Scholar: [Author Only Title Only Author and Title](#)